Buffer-modified C_{60}/pentacene as organic charge generation layer based on Al and MoO_3*

WANG Zhen (王振)**, **LIU Fei** (柳菲), **CHEN Ai** (陈爱), **XIE Jia-feng** (谢嘉凤), **and CHEN Wei-zhong** (陈伟中)

School of Optoelectronic Engineering, Chongqing University of Posts and Telecommunications, Chongqing 400065, China

(Received 30 December 2017; Revised 6 February 2018)

We demonstrate tandem organic light-emitting diodes (TOLEDs) with excellent performance using Al and MoO_3 buffer-modified C_{60}/pentacene as charge generation layer (CGL). Al and MoO_3 were used as the electron and hole injection layers of C_{60}/pentacene CGL, respectively. Green phosphorescence TOLEDs with the structure of ITO/NPB/mCP:Ir(ppy)$_3$/TPBi/Al/C_{60}/pentacene/MoO_3/NPB/mCP:Ir(ppy)$_3$/TPBi/Cs_2CO_3/Al were fabricated. The results show that the inserted Al and MoO_3 can effectively increase the charge injection capacity of organic CGL, resulting the improvement of luminance and current efficiency of TOLEDs. The turn-on voltage of TOLEDs is much lower than that of single-unit device, and the current efficiency is more than 2 times larger than that of the single-unit device. TOLEDs can exhibit excellent photoelectric performance when the thicknesses of Al, C_{60}, pentacene and MoO_3 are 3 nm, 15 nm, 25 nm and 1 nm, respectively. The maximum luminance and current efficiency are 7 920.0 cd/m^2 and 16.4 cd/A, respectively. This work is significant to build new CGL structures for realizing high-performance TOLEDs.

Document code: A **Article ID:** 1673-1905(2018)04-0286-5

DOI https://doi.org/10.1007/s11801-018-7275-y

Tandem organic light-emitting diodes (TOLEDs) have attracted enormous attention over the past decade due to their advantages of high brightness, high efficiency and long lifetime under low current density[1-3]. In 2003, Kido et al[4] firstly proposed the concept of TOLED, they used BCP/V_2O_5 as a transparent layer to connect several light-emitting units. TOLEDs consist of two or more individual light-emitting units connected through charge generation layer (CGL) which can generate electrons and holes in an applied electrical field. The performance of TOLEDs are influenced by the light-emitting units, besides by the CGL[5-7]. Therefore, material selection and structural design of CGL are both key factors to influence the photoelectric performance of TOLEDs. Nowadays, many kinds of CGL have been reported[8-12]. A typical structure of p-n junction is widely researched. The metal oxides, such as V_2O_5[13], MoO_3[8,14] and WO_3[15,16], are used as p-type material. Others are p-doped organic material[11], such as NPB:$FeCl_3$. Low work function metals are doped into electron transport layer material to form n-doped organic material[17,18], such as Alq$_3$:Mg, Bphen:Li, Bphen:Mg, etc. However, fabricating the doped CGL complicates the experimental processes and increases the production cost by the co-evaporation or magnetron sputtering technology. Because most of n-type dopants are active metals (e.g. Li, Mg), doping them is not easy to control at low concentration in a vacuum evaporation system. Therefore, it is necessary and important to study non-doped CGL.

In this paper, we design and fabricate a series of inverted structure non-light-emitting devices to prove that C_{60}/pentacene can effectively generate charge. Because of the excellent electronic transport characteristics and electrical conductivity, C_{60} has attracted significant attention recently and is widely used in OLED and solar cells. The n-type organic semiconductor C_{60} and the p-type organic semiconductor pentacene constitute charge generation layer, which is an important part of tandem devices. Then based on C_{60}/pentacene CGL, the effect of Al and MoO_3 on TOLEDs is studied. It is found that the maximum current efficiencies of TOLEDs using C_{60}/pentacene and Al/C_{60}/pentacene/MoO_3 as the non-doped CGL are 1.2 and 3 times larger than that of a single-unit device, respectively. Furthermore, compared with the C_{60}/pentacene CGL device, the current efficiency of Al/C_{60}/pentacene/MoO_3 CGL device is

* This work has been supported by the National Natural Science Foundation of China (No.61604027), the Basic and Advanced Technology Research Project of Chongqing Municipality (Nos.cstc2016jcyjA0272 and cstc2016jcyjA2063), the Scientific and Technological Research Foundation of Chongqing Municipal Education Commission (Nos.KJ1500424 and KJ1600418), and the Youth Natural Science Foundation of Chongqing University of Posts and Telecommunications (No.A2013-39).

** E-mail: wangzhen@cqupt.edu.cn

improved by 77%, because of the efficient charge generation and injection capability of Al and MoO_3 modified C_{60}/pentacene. Theses advantageous properties provide insights into high-performance structured TOLEDs.

The glass substrate precoated with indium tin oxide (ITO) layer (with thickness of 180 nm, T≥84% and $R_{\square}$≤7 Ω/□) was used as the growth substrate. Before organic film deposition, the ITO-coated substrates were cleaned with ethanol and acetone (the order is ethanol→acetone→ethanol→3 times deionized water), then dried in an oven, and finally treated with oxygen plasma before loaded into a vacuum evaporation system with a base pressure below 5.0×10^{-5} Torr. The thickness of films was monitored with a calibrated quartz thickness monitor. The deposition rates of organic materials and Al as cathode were 0.1 nm/s and 0.3 nm/s, respectively. The electroluminescent (EL) spectra, luminance-voltage and current-voltage characteristics were measured by using the photoelectric test system consisting of PR670 SpectraScan spectrometer and Keithley2450 voltage current source. The transmittance was measured by a Carry5000 Spectrophotometer. All measurements were carried out at room temperature under ambient conditions.

A series of inverted structure non-light-emitting devices were designed to understand the charge generation principle of CGL. The electron transporting layer (ETL) N-arylbenzimidazoles (TPBi) is deposited on ITO, and then the CGL, N, N′-bis-(1-naphthyl)-N,N′-diphenyl-1, 1′-biphenyl-4,4′-diamine (NPB) and Al cathode are grown. There is no CGL in the comparison device. For optimizing the thickness of CGL, the structures of devices are as follows: ITO/TPBi/NPB/Al and ITO/TPBi/C_{60}/pentacene/NPB/Al with different thicknesses of C_{60} and pentacene. Then, $Ir(ppy)_3$ is a green phosphor material, N,N'-dicarbazolyl-3,5-benzene (mCP): $Ir(ppy)_3$ is used as light-emitting cell to fabricate TOLEDs and the comparison single-unit device. The structures of TOLEDs devices are ITO/NPB/mCP:$Ir(ppy)_3$/TPBi/Cs_2CO_3/Al, ITO/NPB/mCP:$Ir(ppy)_3$/TPBi/C_{60}/pentacene/NPB/mCP:$Ir(ppy)_3$/TPBi/Cs_2CO_3/Al and ITO/NPB/mCP:$Ir(ppy)_3$/TPBi/Al/C_{60}/pentacene/MoO_3/NPB/mCP:$Ir(ppy)_3$/TPBi/Cs_2CO_3/Al. In order to obtain a device with low driving voltage and high current efficiency, we change the Al thickness in the structure of ITO/NPB/mCP:$Ir(ppy)_3$/TPBi/Al(y nm)/C_{60}/pentacene/MoO_3/NPB/mCP:$Ir(ppy)_3$/TPBi/Cs_2CO_3/Al.

The structure of device A_1 is ITO/TPBi(40 nm)/NPB(40 nm)/Al(100 nm), and the structures of device A_2—A_6 are ITO/TPBi(40 nm) /C_{60}(x nm)/pentacene (40−x nm)/NPB(40 nm) /Al(100 nm) with x=0, 5, 10, 15 and 20, respectively. Fig.1 shows the current density-voltage (*J-V*) characteristic curves of devices A_1—A_6. Obviously, there is current in the inverted devices A_3—A_6 with the C_{60}/pentacene CGL, but the current density is almost zero in the devices A_1 and A_2 without the complete CGL. Because the highest occupied molecular orbital (HOMO) of ITO anode (~4.8 eV) is much lower than that of TPBi (~6.1 eV), and the lowest unoccupied molecular orbital (LUMO) of Al cathode (~4.0 eV) is much higher than that of NPB (~2.4 eV). Holes and electrons generated by the anode and cathode are difficultly transported from TPBi and NPB to the cathode and anode, respectively. However, when the CGL is added into inverted devices, the charge from CGL can be easily injected into electrode through ETL TPBi and HTL NPB, because the LUMO of C_{60} (~4.5 eV) is close to that of TPBi (~2.8 eV), as well as the HOMO of pentacene (~4.9 eV) and NPB (~5.5 eV). The schematic diagrams of the corresponding inverted devices are shown in Fig.2. It is observed that the device A_5 has optimal performance when the thicknesses of C_{60} and pentacene are 15 nm and 25 nm, respectively.

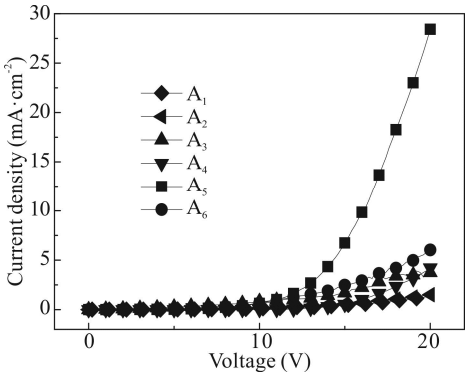

Fig.1 *J-V* characteristic curves of devices A_1—A_6

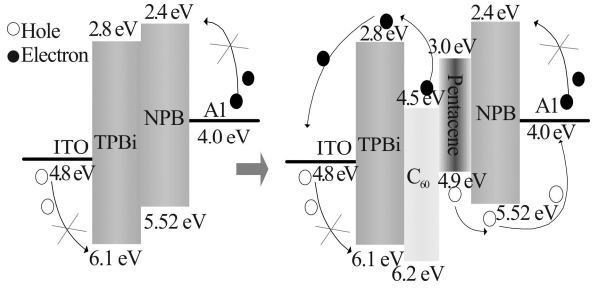

Fig.2 Schematic diagrams of the inverted devices

Then MCP:$Ir(ppy)_3$ is used as light-emitting cell to fabricate single-unit device B_1 with structure of ITO/NPB (40 nm)/mCP:8 wt% $Ir(ppy)_3$ (30 nm)/TPBi (40 nm)/Cs_2CO_3 (1 nm)/Al (100 nm), TOLED B_2 with structure of ITO/NPB (40 nm)/mCP:8 wt% $Ir(ppy)_3$ (30 nm)/TPBi (20 nm)/C_{60} (15 nm)/pentacene (25 nm)/NPB (20 nm)/mCP:8 wt% $Ir(ppy)_3$ (30 nm)/TPBi (40 nm)/Cs_2CO_3 (1 nm)/Al (100 nm) and TOLED B_3 with structure of ITO/NPB (40 nm)/mCP:8 wt% $Ir(ppy)_3$ (30 nm)/TPBi (20 nm)/Al (1 nm)/C_{60} (15 nm)/pentacene (25 nm)/MoO_3 (1 nm)/NPB (20 nm)/mCP:8 wt% $Ir(ppy)_3$ (30 nm)/TPBi (40 nm)/Cs_2CO_3 (1 nm)/Al (100 nm).

Figs.3 and 4 show the current density-voltage- luminance (*J-V-L*) and the efficiency-current density (*E-J*) characteristic curves of devices B_1—B_3. As shown in

Fig.3, at the same current density and luminance, B_2 and B_3 have a higher operating voltage compared with the B_1. Furthermore, the turn-on voltage and operating voltage are significantly within 2 times of those of B_1, which is a great significance for effectively improving the power efficiency of the TOLEDs. The turn-on voltages of B_2 and B_3 are 10.7 V and 9.7 V, which are 1.6 times and 1.4 times larger than that of B_1 (6.8 V), respectively. *L-V* characteristic curve can also clearly describe the above phenomenon. At a luminance of 900 cd/m^2, the operating voltages of B_2 and B_3 are 14.3 V and 16.8 V, respectively, which are 2 times lower than that of B_1 (15.2 V). We find turn-on voltage and operating voltage values of B_3 are smaller than those of B_2, which demonstrates the CGL with Al and MoO_3 layer is better. As shown in Fig.4, the maximum current efficiencies of B_2 and B_3 are 7.2 cd/A and 12.8 cd/A, which are 2.2 times and 4.0 times larger than that of B_1 (3.2 cd/A), respectively. And the maximum current efficiency of B_3 is improved by nearly 77% compared with that of B_2. Therefore, Al/C_{60}/pentacene/MoO_3 is an efficient CGL with better charge generation and separation capability, which can greatly improve the photoelectric performance of TOLED. The performance related parameters of devices B_1—B_3 are shown in Tab.1.

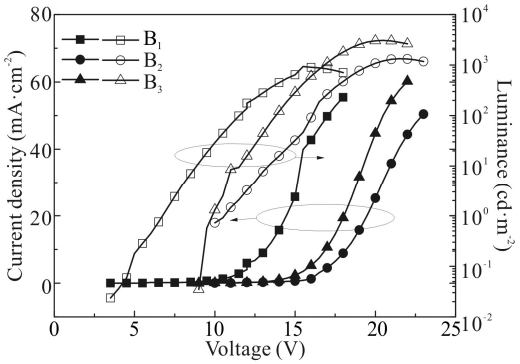

Fig.3 *J-V-L* characteristic curves of devices B_1—B_3

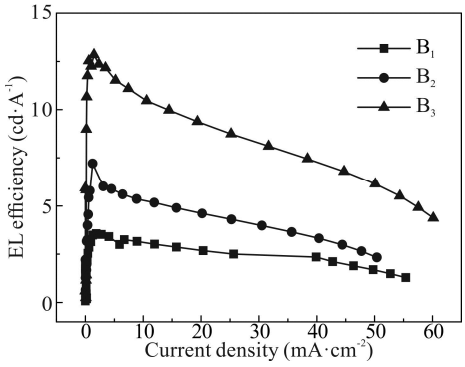

Fig.4 *E-J* characteristic curves of devices B_1—B_3

Tab.1 The performance parameters of devices B_1—B_3

Device	B_1	B_2	B_3
Turn-on voltage at 1 cd·m^{-2} (V)	6.8	10.7	9.7
Operating voltage at 900 cd·m^{-2} (V)	15.2	14.3	16.8
Luminance at 10 mA·cm^{-2} (cd·m^{-2})	360.4	612.5	1 110.0
Maximum luminance (cd·m^{-2})	935.0	1 338.0	3 076.5
Maximum EL efficiency (cd·A^{-1})	3.2	7.2	12.8

In order to achieve optimal performance of TOLED, a series of devices with different thickness of Al were designed to explore the impact of Al layer thickness on the performance of TOLEDs, i.e., devices C_1—C_4 with structure of ITO/NPB (40 nm)/mCP:8 wt% Ir(ppy)$_3$ (30 nm) /TPBi (20 nm)/Al (*y* nm)/C_{60} (15 nm)/pentanece (25 nm)/MoO_3 (1 nm)/NPB (20 nm)/mCP:8 wt% Ir(ppy)$_3$ (30 nm)/TPBi (40 nm)/Cs_2CO_3 (1 nm)/Al (100 nm) with *y*=1, 3, 5 and 7, respectively.

Figs.5 and 6 show *J-V-L* and *E-J* characteristic curves of devices C_1—C_4. From Fig.5, the luminance and current efficiency of TOLEDs increase, and the turn-on voltage decrease with increase of the thickness of Al. At the current density of 10 mA/cm^2, the luminance values of C_2 and C_3 increase compared with that of C_1, but that of C_4 decreases, because Al layer of C_4 is so thick that it causes a decrease in transmittance. The maximum current efficiency of devices C_2 and C_3 are 16.4 cd/A and 16.6 cd/A, respectively, which are increased by 28% and 30% compared with that of C_1. In this study, Al/C_{60}/pentacene/MoO_3 as CGL effectively reduces the operating voltages of the devices. Because in an electric field, electrons go across the low barrier along the LUMO of C_{60} and are injected into the Al layer. On the other hand, MoO_3 used in CGL is a p-type metal oxide material with *T*>80%. Its HOMO (~5.3 eV) is quite close to that of NPB (~5.5 eV), so that the holes stored in the interface can be easily injected into the light-emitting cell. This structure reduces the charge injection potential barrier, as well as turn-on voltage and operating voltage of devices. The performance related parameters of devices C_1—C_4 are shown in Tab.2.

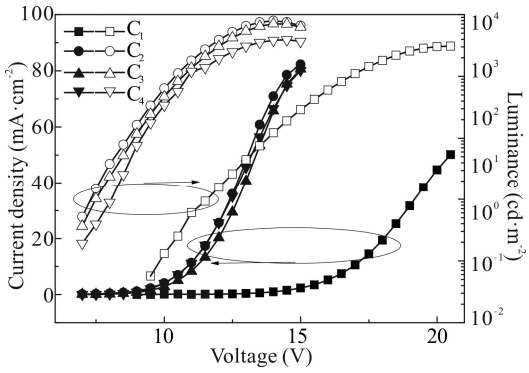

Fig.5 *J-V-L* characteristic curves of devices C_1—C_4

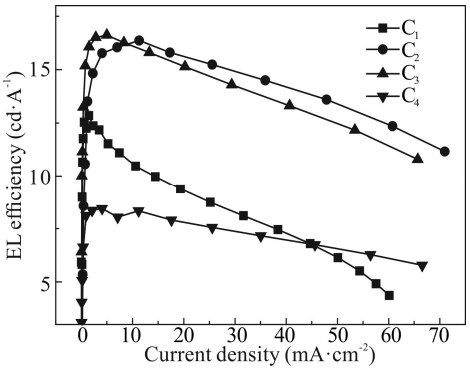

Fig.6 *E-J* characteristic curves of devices C_1—C_4

Tab.2 The performance parameters of devices C_1—C_4

Device	C_1	C_2	C_3	C_4
Turn-on voltage at 1 cd·m^{-2} (V)	9.7	6.5	5.9	6.3
Operating voltage at 3 000 cd·m^{-2} (V)	16.8	11.8	12.0	12.7
Luminance at 10 mA·cm^{-2} (cd·m^{-2})	1 110.0	1 791.6	1 650.5	1 203.4
Maximum luminance (cd·m^{-2})	3 076.5	7 920.0	7 085.5	3 906.0
Maximum EL efficiency (cd·A^{-1})	12.8	16.4	16.6	8.3

As shown in Figs.5, 6 and Tab.2, devices C_2 and C_3 exhibit optimal performance. The normalized EL spectra of the single-unit device and the TOLEDs, and the lighting diagram of the TOLEDs are shown in Figs.7 and 8, respectively. It can be seen clearly that the peak of emission band is at 510 nm. Additionally, the transparencies of Al with variable thicknesses are different in the visible light range, so each material layer of the device should have high light transmittance to acquire high efficient TOLEDs. Fig.9 shows the transmittance spectra of TOLEDs with different thicknesses of Al from 0 nm to 9 nm. It can be distinctly observed that the transmittance increases with decrease of the thickness of Al. However, the performance of the device weakens for thinner Al layer. The average transmittance values are larger than 90% when the thicknesses of Al layers are 1 nm and 3 nm, respectively. And the average transmittance of TOLED with 5-nm-thick Al is only approximately 80%. At the wavelength of 512 nm, the transmittance values of TOLEDs with 3-nm-thick and 5-nm-thick Al are 90.8%, 77.2%, respectively. So Al layer with thickness of 3 nm is better than that of 5 nm. The results show that as the thickness of Al is 3 nm, the performance of the device C_2 is optimization with CGL structure of Al (3 nm)/C_{60} (15 nm)/pentacene (25 nm)/MoO_3 (1 nm).

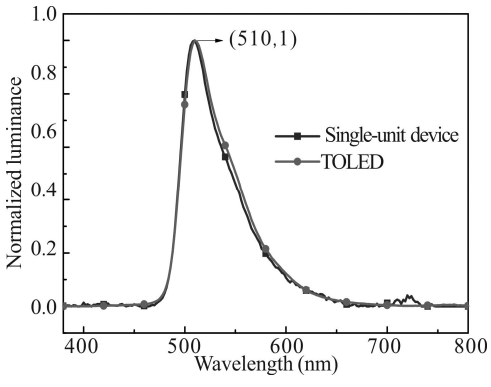

Fig.7 The EL spectra of the single-unit device and the TOLEDs

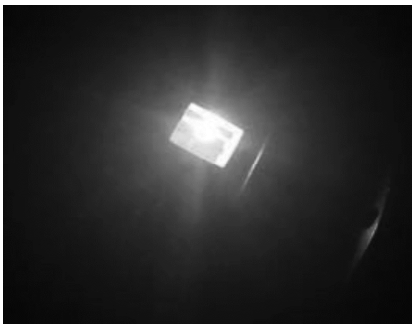

Fig.8 The lighting diagram of the TOLEDs

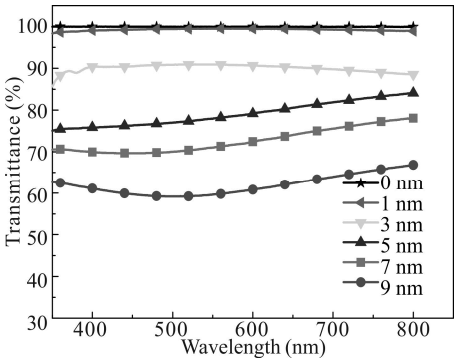

Fig.9 Transmittance spectra of TOLEDs with different Al thicknesses from 0 nm to 9 nm

In summary, we develop a multilayer structure of Al/C_{60}/pentacene/MoO_3 as CGL for TOLEDs, where both Al and MoO_3 are used as charge injection layers. Al and MoO_3 buffer-modified C_{60}/pentacene as CGL is investigated to achieve effective performance of TOLEDs. The results show that inserting Al and MoO_3 can effectively improve charge injection capacity of organic CGL, resulting in increasing luminance and current efficiency of TOLEDs. The turn-on voltage of TOLEDs is significantly lower than that of single-unit device, and the current efficiency is more than 2 times larger than that of single-unit device. TOLED can deliver optimal photoelectric performance when the thicknesses of Al, C_{60}, pentacene and MoO_3 are 3 nm, 15 nm, 25 nm and 1 nm, respectively, and its maximum luminance and current efficiencies are 7 920.0 cd/m^2 and 16.4 cd/A, respectively. This work is significant for designing new CGL structures for achieving efficient CGL and TOLED.

References

[1] Zhang X, Zhang M, Liu M, Chen Y, Wang J, Zhang X, Zhang J, Lai W Y and Huang W, Organic Electronics **53**, 353 (2018).

[2] Yang H, Yu Y, Wu L, Qu B, Lin W, Yu Y, Wu Z and Xie W, Applied Physics Express **11**, 022101 (2018).

[3] Fung M K, Li Y Q and Liao L S, Advanced Materials **28**, 10381 (2016).

[4] Kido J, Matsumoto T, Nakada T, Endo J, Mori K, Ka-

wamura N and Yokoi A, SID Symposium Digest of Technical Papers **34**, 964 (2003).

[5] Chen Y H, Chen J S, Ma D G, Yan D H, Wang L X and Zhu F R, Applied Physics Letters **98**, 114 (2011).

[6] Bi W T, Wu X M, Hua Y L, Sun J E, Xiao Z H, Wang L and Yin Shou-Gen. [J]. Chinese Physics B **23**, 017803 (2013). (in Chinese)

[7] Lu F P, Wang Q and Zhou X, Chinese Physics B **22**, 037202 (2013). (in Chinese)

[8] Liu Y, Wu X, Xiao Z, Gao J, Zhang J, Rui H, Lin X, Zhang N, Hua Y and Yin S, Applied Surface Science **413**, 302 (2017).

[9] Jin T C, Kim D H, Koh E I and Kim T W, Thin Solid Films **570**, 63 (2014).

[10] Yang J, Suman C K, Kim J, Song W J, Wooh S, Char K and Lee C, Journal of Nanoscience and Nanotechnolgy **14**, 5898 (2014).

[11] Wu Y K, Sun Y, Qin H Y, Hu S C, Wu Q Y and Zhao Y, Synthetic Metals **228**, 45 (2017).

[12] Wu Y K, Sun Y, Qin H Y, Hu S C, Wu Q Y and Zhao Y, Applied Physics A Materials Science & Processing **123**, 234 (2017).

[13] Tsutsui T and Terai M, Applied Physics Letters **84**, 440 (2004).

[14] Yang H, Kim J, Yamamoto K and Hosono H, Organic Electronics **46**, 133 (2017).

[15] Qin D, Zhao W, Chen L, Shi Z and Cao H, Journal of the Society for Information Display **25**, 337 (2017).

[16] Ho fle S, Bernhard C, Bruns M, Kübel C, Scherer T, Lemmer U and Colsmann A, ACS Applied Materials & Interfaces **7**, 8132 (2015).

[17] Yu Y, Wu Z, Yu Y, Lin W, Yang H and Chen P, Organic Electronics **52**, 329 (2018).

[18] Lei Y, Liu Z, Fan C J, Peng X F, Ji X X, Li G Q, Xiong Z H and Yang X H, The Journal of Physical Chemistry C **121**, 793 (2017).